

Mesoscopic entanglement induced by spontaneous emission in solid-state quantum optics

Article (Published Version)

González-Tudela, Alejandro and Porras, Diego (2013) Mesoscopic entanglement induced by spontaneous emission in solid-state quantum optics. *Physical Review Letters*, 110 (8). 080502. ISSN 0031-9007

This version is available from Sussex Research Online: <http://sro.sussex.ac.uk/id/eprint/46124/>

This document is made available in accordance with publisher policies and may differ from the published version or from the version of record. If you wish to cite this item you are advised to consult the publisher's version. Please see the URL above for details on accessing the published version.

Copyright and reuse:

Sussex Research Online is a digital repository of the research output of the University.

Copyright and all moral rights to the version of the paper presented here belong to the individual author(s) and/or other copyright owners. To the extent reasonable and practicable, the material made available in SRO has been checked for eligibility before being made available.

Copies of full text items generally can be reproduced, displayed or performed and given to third parties in any format or medium for personal research or study, educational, or not-for-profit purposes without prior permission or charge, provided that the authors, title and full bibliographic details are credited, a hyperlink and/or URL is given for the original metadata page and the content is not changed in any way.

Mesoscopic Entanglement Induced by Spontaneous Emission in Solid-State Quantum Optics

Alejandro González-Tudela¹ and Diego Porras²

¹*Departamento de Física Teórica de la Materia Condensada, Universidad Autónoma de Madrid, 28040 Madrid, Spain*

²*Departamento de Física Teórica I, Universidad Complutense, 28040 Madrid, Spain*

(Received 21 September 2012; revised manuscript received 29 November 2012; published 20 February 2013)

Implementations of solid-state quantum optics provide us with devices where qubits are placed at fixed positions in photonic or plasmonic one-dimensional waveguides. We show that solely by controlling the position of the qubits and with the help of a coherent driving, collective spontaneous decay may be engineered to yield an entangled mesoscopic steady state. Our scheme relies on the realization of pure superradiant Dicke models by a destructive interference that cancels dipole-dipole interactions in one dimension.

DOI: [10.1103/PhysRevLett.110.080502](https://doi.org/10.1103/PhysRevLett.110.080502)

PACS numbers: 03.67.Bg, 03.67.Ac, 37.10.Ty, 37.10.Vz

The study of atoms coupled to the electromagnetic (EM) field confined in cavities or optical waveguides has played a central role in the fields of quantum optics and atomic physics. In recent years the basics of that physical system have been realized with artificially designed atoms in solid-state setups. We may include here quantum dots and nitrogen vacancy (NV) centers deterministically coupled to photonic cavities [1–3], and plasmonic [4,5] or photonic [6–10] waveguides, as well as circuit QED setups where superconducting qubits are coupled to microwave cavities [11,12]. Even though the physics of atomic and solid-state quantum optical systems is similar, the latter show a crucial advantage: on a solid substrate, emitters may be placed permanently at fixed positions at separations of the order of relevant wavelengths [13]. An important application of those systems is quantum information processing in solid-state devices [14], where artificial atoms acting as qubits are placed within the EM field confined in a microcavity. Typically, the realization of those ideas requires unitary qubit-field evolutions induced by collective couplings to a single mode in a cavity. An alternative pathway is to tailor the interaction with the environment to induce quantum correlations between qubits with dissipation [15,16]. This approach has been proven to be advantageous to generate entanglement between ensembles of atoms [17]. In this direction one-dimensional guided modes have been recently pointed out as a useful tool to create two-qubit entanglement [18–20] and many-qubit entanglement in cascaded quantum networks [21].

In this Letter, we show that by placing a set of qubits in a one-dimensional waveguide (see Fig. 1) the continuum of EM field modes induces a controllable dissipative coupling between the qubits. The possibility of deterministically positioning the artificial atoms or qubits allows us to engineer the paradigm for quantum optical collective effects, i.e., the Dicke model of superradiance [22] in its pure form. The observation of the latter in optical systems is hindered due to dephasing caused by dipole-dipole interactions [23,24]. In our scheme those interactions can be switched off by an appropriate choice of the interqubit

distance. Adding a classical drive to the pure Dicke model we obtain a dissipative system with a phase diagram of steady states showing mesoscopic spin squeezing and entanglement. This model has been theoretically investigated in the past [25–27], but experimental realizations are scarce. Finally we upgrade our scheme to a set of N four-level emitters [28,29] and show that a judicious choice of couplings to the waveguide and dispersion relations may lead to a variety of many-body dissipative models which show entangled steady states.

We start by modeling N two-level systems (2LSs), $\{|g\rangle_n, |e\rangle_n\}_{n=1\dots N}$, placed at positions x_n and coupled to a one-dimensional field [see Fig. 1(a)] with photon annihilation operators a_q , described by the Hamiltonian $H = H_0 + H_I$. The free term is $H_0 = H_{qb} + H_{\text{field}}$, with ($\hbar = 1$)

$$H_{qb} = \frac{\omega_0}{2} \sum_{n=1}^N \sigma_n^z, \quad H_{\text{field}} = \sum_q \omega_q a_q^\dagger a_q, \quad (1)$$

where ω_0 is the qubit energy [see Fig. 1(b)] and ω_q is the field dispersion relation. We define the Pauli matrices

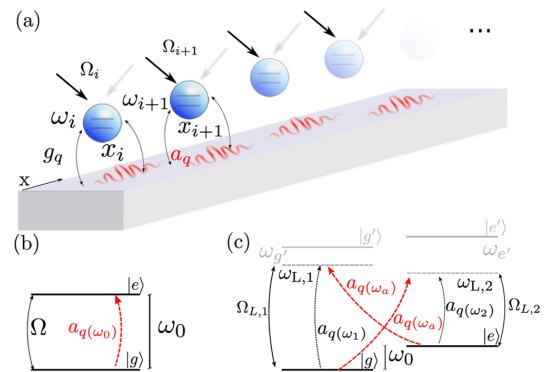


FIG. 1 (color online). Panel (a) Experimental scheme of the system: ensemble of equally spaced qubits placed in the vicinity of a one-dimensional waveguide. Panel (b) Two-level system configuration with resonant excitation. Panel (c): Four-level system configuration with two additional lasers, where we impose the condition: $\omega_{L,1} - \omega_0 = \omega_{L,2} + \omega_0 = \omega_a$ and define $\omega_1 = \omega_{L,1}$, $\omega_2 = \omega_{L,2} - \omega_0$.

$\sigma_n^z = |e\rangle_n\langle e| - |g\rangle_n\langle g|$, $\sigma_n^+ = |e\rangle_n\langle g|$, $\sigma_n^- = |g\rangle_n\langle e|$. The photon polarization is neglected to focus on the most relevant physics of our work. We consider a dipolar coupling of the form

$$H_I = \sum_n [\sigma_n E(x_n) + \text{H.c.}] \quad (2)$$

with $E(x) = \sum_q g_q (a_q e^{iqx} + a_q^\dagger e^{-iqx})$, and g_q a dipolar qubit-field coupling. We define ρ as the reduced density matrix for the qubits. In the weak coupling limit, the evolution of ρ can be described by a Markovian master equation of the form $d\rho/dt = \mathcal{L}(\rho)$ [30], with the superoperator

$$\mathcal{L}(\rho) = \sum_{n,m} J_{n,m} (\sigma_n^- \rho \sigma_m^+ - \rho \sigma_m^+ \sigma_n^-) + \text{H.c.} \quad (3)$$

A detailed derivation follows the description in dimensions higher than one presented in previous works [24] (see Sec. A of the Supplemental Material [31]). Special care must be paid to the counter rotating terms in Eq. (3), which have to be included to get the following result for the collective decay rates

$$J_{n,m} = \frac{\Gamma}{2} e^{iq(\omega_0)|x_n - x_m|}. \quad (4)$$

We define $\Gamma = \gamma(\omega_0)$, with the function $\gamma(\omega) = g_{q(\omega)}^2 D(\omega)/\pi$, where $q(\omega)$ is the resonant wave vector at ω , and we have defined the EM density of states, $D(\omega) = (2\pi/L)|dq(\omega)/d\omega|$, with L the quantization length. A crucial observation for this work is that the couplings $J_{n,m}$ ideally do not decay with distance, a situation that is unique to one-dimensional waveguides. In free space, on the contrary, collective couplings decay like $1/r$ or $1/r^3$, depending on the relative dipole orientation [24].

Homogeneous couplings [18,19,32–34] $J_{n,m} = \Gamma/2$ can be obtained from Eq. (4) by the choice $x_n = n\lambda_0$, with $\lambda_0 = 2\pi/q_0$, and $n \in \mathbb{Z}$. This condition cancels dipole-dipole interactions and we get the pure Dicke superradiant decay described by

$$\mathcal{L}_D(\rho) = \frac{\Gamma}{2} (S^- \rho S^+ - S^+ S^- \rho) + \text{H.c.}, \quad (5)$$

with $S^- = \sum_n \sigma_n^-$, $S^+ = \sum_n \sigma_n^+$. We also define $S_\alpha = \sum_n \sigma_n^\alpha/2$, ($\alpha = x, y, z$), and the basis $\{|J, M\rangle\}$ of eigenstates of \vec{S}^2 , S_z . Assuming an initial state like $|\Psi_0\rangle = \otimes_n |e\rangle_n = |N/2, N/2\rangle$ the system evolves within the sector $J = N/2$. We note that Dicke superradiant decay is achieved in one dimension without the restriction that the whole qubit ensemble is confined within a region of length λ_0 , which is a requirement for other realizations, i.e., atomic ensembles.

In this Letter we focus on the qubit steady state, ρ_s , which for a given Liouvillian fulfills $\mathcal{L}(\rho_s) = 0$. To achieve some controllability on ρ_s , we add a pump term which physically can be implemented by the interaction of qubits with a resonant field with Rabi frequency Ω ,

$$\mathcal{L}_{D,p}(\rho) = \mathcal{L}_D(\rho) - i\frac{\Omega}{2}[S_x, \rho]. \quad (6)$$

Competition between the collective decay and the pumping leads to a nonequilibrium phase transition in the steady state of the model at a critical pumping rate $\Omega_c = N\Gamma/2$ [25], manifested in a kink in the population inversion observable $\langle S_z \rangle$ [see Fig. 2(a)]. Let us first give a brief description of the two limiting cases. (i) Coherent steady state regime, $\Omega \ll N\Gamma/2$. Since $\mathcal{L}_{D,p}$ can be obtained from \mathcal{L}_D by the substitution $S^- \rightarrow S^- + i\Omega/(2\Gamma)$, one can easily show that $\rho_s = |\Psi_c\rangle\langle\Psi_c| + \mathcal{O}^2(\frac{\Omega}{\Gamma})$, where $|\Psi_c\rangle = e^{i\frac{\Omega}{2}S_x}|N/2, -N/2\rangle$ is a spin coherent state. (ii) The mixed state phase, $\Omega \gg N\Gamma/2$. Here we get an infinite temperature state. To show this, it is convenient to write \mathcal{L}_D in the interaction picture with respect to $\Omega S_x/2$. This allows us to make the replacement $S^- \rightarrow S_x + (1/2)[\cos(t)S_y + \sin(t)S_z]$. Averaging over time, leads to

$$\mathcal{L}_{D,p} \approx \frac{\Gamma}{2} \left(S_x \rho S_x - S_x^2 \rho + \frac{1}{2} \sum_{\alpha=y,z} (S_\alpha \rho S_\alpha - S_\alpha^2 \rho) \right) + \text{H.c.}, \quad (7)$$

which has the infinite temperature state $\rho_s = \mathbf{1}$ as the steady state. For calculations in the intermediate regime we use the full solution in the $|J, M\rangle$ basis.

To quantify the entanglement we use the spin squeezing ξ as a figure of merit,

$$\xi^2 = \frac{N(\Delta S_x)^2}{\langle S_y \rangle^2 + \langle S_z \rangle^2}. \quad (8)$$

The latter is both an entanglement witness and it is also linked to applications in quantum metrology [35–37]. Symmetric multiqubit states with $\xi < 1$ can be shown to be entangled [36] with pairwise entanglement between any pair of qubits [38]. Note that the above mentioned phases (i) and (ii) lead to $1/\xi^2 = 1$ and $1/\xi^2 = 0$, respectively. Another theoretical tool to be used is the purity, defined by $\mathcal{P}(\rho) = \text{Tr}(\rho^2)$, although we note that ξ witnesses entanglement also for mixed states. Both magnitudes are plotted for increasing number of qubits N in Fig. 2. We find a range of pumping fields ($\Omega \leq \Omega_c$) that induce a pure entangled ρ_s . This result leads to the controllable generation of entangled states in mesoscopic samples of artificial atoms. The time scale needed to achieve the stationary entangled states benefits from a collective enhancement scaling as ΓN , so that the higher the number of qubits, the more efficient is the preparation of states.

We now upgrade our 2LS into a four-level system (4LS) configuration [see Fig. 1(c)], and show that this is a more advantageous situation. Our scheme can be realized in the solid-state context [28,29] and describes a variety of possible configurations in which a set of low-level states are coupled to excited states by lasers with different polarizations. Two ground states ($|g\rangle_n, |e\rangle_n$) are coupled to high energy states ($|g'\rangle_n, |e'\rangle_n$). The qubit part of the free Hamiltonian becomes now

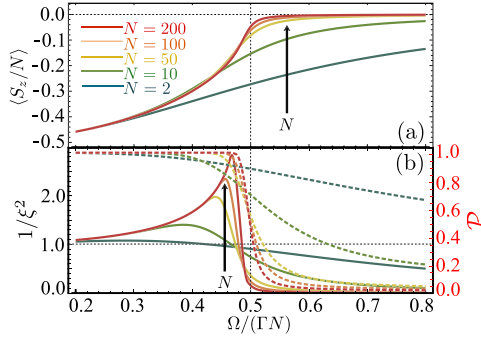


FIG. 2 (color online). Numerical results for the coherently pumped Dicke model [Eq. (6)] for increasing N . Different colors represent different number of qubits from $N = 2$ to $N = 200$ as shown in the legend. (a) Population inversion $\langle S_z \rangle / N$. (b) Purity \mathcal{P} (dashed) and spin-squeezing parameter $1/\xi^2$ (solid).

$H_{qb} = \sum_n (\omega_{g'} |g'\rangle_n \langle g'| + \omega_{e'} |e'\rangle_n \langle e'| + \omega_g |g\rangle_n \langle g|)$. Two weak nonresonant fields with amplitudes $\Omega_{L,1(2)}$ and frequencies $\omega_{L,1(2)}$, induce transitions described by a Hamiltonian term $H_L = \sum_n [(\Omega_{L,1}/2) |e'\rangle_n \langle e| e^{-i\omega_{L,1}t} + (\Omega_{L,2}/2) |g'\rangle_n \langle g| e^{-i\omega_{L,2}t} + \text{H.c.}]$. We impose the condition $\omega_{L,1} - \omega_0 = \omega_{L,2} + \omega_0 = \omega_a$, such that the two decay channels in red of Fig. 1(c) (into modes a_q) correspond to photon emission with the same energy ω_a . After an adiabatic elimination of the excited states (see Sec. II of the Supplemental Material [31] for details) we get an effective qubit-field interaction $H_I(t) = H_I^{sq}(t) + H_I^z(t)$, written in the interaction picture with respect to H_0 . The first term reads

$$H_I^{sq}(t) = \sum_n \kappa E(x_n, t) (D_n^\dagger e^{i\omega_a t} + D_n e^{-i\omega_a t}), \quad (9)$$

where $\kappa^2 = (\Omega_{L,1}/2\Delta_1)^2 - (\Omega_{L,2}/2\Delta_2)^2$ ($\Delta_{1(2)} = \omega_{e'(g')} - \omega_{L,1(2)}$) is a normalization constant. $D_n = u\sigma_n^- + v\sigma_n^+$ is a jump operator resulting from the cross radiative decay, with $u = \kappa^{-1}\Omega_{L,1}/2\Delta_1$ and $v = \kappa^{-1}\Omega_{L,2}/2\Delta_2$, fulfilling $u^2 - v^2 = 1$. The latter condition will be useful in the discussion below, and allows characterization by a single parameter r , such that $u = \cosh(r)$, $v = \sinh(r)$. After eliminating the EM field degrees of freedom we arrive at the Liouvillian

$$\mathcal{L}_{sq}(\rho) = \sum_{n,m} J_{n,m}^{sq} (D_n^- \rho D_m^+ - \rho D_m^+ D_n^-) + \text{H.c.} \quad (10)$$

with $J_{n,m}^{sq} = \Gamma_{sq} e^{iq(\omega_a)|x_n - x_m|}$ and $\Gamma_{sq} = \kappa^2 \gamma(\omega_a)$. The second term in the effective qubit-field interaction describes the longitudinal decay processes

$$H_I^z(t) = \kappa \sum_n E(x_n, t) (u\sigma_n^z e^{i\omega_1 t} + v\sigma_n^z e^{-i\omega_2 t} + \text{H.c.}), \quad (11)$$

and leads to

$$\mathcal{L}_z(\rho) = \sum_{n,m} J_{n,m}^z (\sigma_n^z \rho \sigma_m^z - \rho \sigma_m^z \sigma_n^z) + \text{H.c.} \quad (12)$$

with $J_{n,m}^z = \kappa^2 [\gamma(\omega_1) u^2 e^{iq(\omega_1)|x_n - x_m|} + \gamma(\omega_2) v^2 e^{iq(\omega_2)|x_n - x_m|}]$ where $\omega_1 = \omega_{L,1}$ and $\omega_2 = \omega_{L,2} - \omega_0$. The term \mathcal{L}_z induces a dephasing mechanism that competes with the

spontaneous coherence buildup induced by \mathcal{L}_{sq} . The relative importance of those contributions depends on the photon density of states at frequencies ω_a and $\omega_{1,2}$. We consider two limiting cases. (i) Small photonic bandwidth. This is the most favorable configuration. We assume that the density of states in the waveguide is peaked around ω_a , with a bandwidth $\Delta\omega \ll |\omega_1 - \omega_a|, |\omega_2 - \omega_a|$ such that $\gamma(\omega_{1,2}) \approx 0$ and therefore $J_{n,m}^z \approx 0$. For example, this can be the case of one-dimensional waveguides consisting of coupled cavities forming a one-dimensional photonic crystal. Defining $q(\omega_a) = 2\pi/\lambda_a$ and choosing $x_n = n\lambda_a$ we arrive at a spin-squeezed version of the Dicke superradiant model

$$\mathcal{L}_{sq,D}(\rho) = \frac{\Gamma_{sq}}{2} (D^- \rho D^+ - D^+ D^- \rho + \text{H.c.}), \quad (13)$$

where we have introduced the collective spin-squeezed operators $D^{+/-} = \sum_n D_n^{+/-}$. In Fig. 3(a) we present a calculation of the spin squeezing in the steady state as a function of the squeezing parameter r . Remarkably, we observe an enhancement of the maximum value of the entanglement of several orders of magnitude compared to the case of an ensemble of 2LSs. (ii) A large photonic bandwidth. In the opposite limit we consider a broadband waveguide [18,32] ($|\omega_{L,1} - \omega_{L,2}| \ll \Delta\omega$) such that the density of states at the frequencies considered here is comparable $\gamma(\omega_1) \approx \gamma(\omega_2)$. In experiments with optical transitions, for example with quantum dots in optical or plasmonic waveguides, the condition $\omega_1, \omega_2, \omega_a \gg \omega_0$ is found, since the transition energies are in the eV and meV ranges for high energy and low energy transitions, respectively [28,29]. Thus, we can safely assume $q(\omega_a) \approx q(\omega_1) \approx q(\omega_2) = 2\pi/\lambda_a$, and consider that quantum dots can be placed at the same relative optical path with respect to all frequencies. To give a more quantitative argument for this approximation we define the group velocity of the modes of the waveguide $v_g(\omega) = |\partial_\omega q|$, and consider the limit $|\omega_1 - \omega_a| v_g(\omega_a), |\omega_2 - \omega_a| v_g(\omega_b) \ll q(\omega_a)$, which corresponds to small wave vector differences. In the case of constant v_g and optical transitions, this condition leads to differences of 10^{-3} in $q(\omega_a), q(\omega_{1,2})$. We neglect for the moment those differences, which may lead to the inhomogeneous broadening effects that are discussed later in this Letter. Thus, the condition $x_n = n\lambda_a$ leads to a collective dephasing term of the form

$$\mathcal{L}_{z,D}(\rho) = \frac{\Gamma_z}{2} (S^z \rho S^z - S^z \rho + \text{H.c.}), \quad (14)$$

where we have introduced the rate $\Gamma_z = J_{n,n}^z$. In the large photonic bandwidth limit we get thus two competing terms $\mathcal{L} = \mathcal{L}_{sq,D} + \mathcal{L}_{z,D}$. Collective dephasing increases with the squeezing parameter r , as depicted in solid black in Fig. 3(b). The competition between the dephasing and squeezing mechanisms determines an optimal r to generate maximal entanglement. The latter can be higher than the one generated by $\mathcal{L}_{D,p}$ in the 2LS scheme considered

above. The large bandwidth limit is a worst-case scenario as typically the waveguide modes are peaked around a certain energy chosen by fabrication. Thus, in the realistic case the entanglement generation will be in a situation between the two limits. The purity of the system is also affected by the dephasing term; however, one can still find a region that combines high purity and high values of entanglement as shown in Fig. 3(b).

Finally, we discuss the feasibility of our ideas, focusing on the following points. (i) One-dimensional waveguides. We require a long propagation length and efficient coupling to the qubits. Coupling to guided modes of 85% to 89% has been reported for photonic [9,10] and plasmonic [4,5] waveguides. Theoretical predictions of even higher efficiencies have been pointed out [32,39], although at the expense of reducing the field propagation length. In addition, the precise location of the qubits is also required, which is possible for solid-state emitters using, i.e., lithographic methods which nowadays have a precision larger than 50 nm [13]. (ii) Lambda transitions in solid-state qubits. We assume a degree of addressability of electronic levels similar to the one achieved in atomic physics, especially the 4LS scheme. Applications in quantum information processing [14,40] typically require controlling optical transitions for spin pumping and initialization.

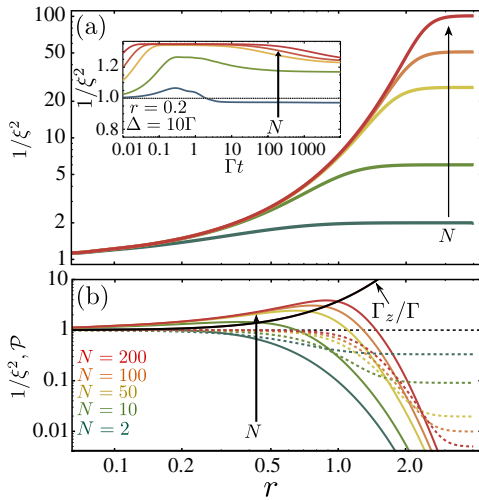


FIG. 3 (color online). Entanglement witness for the 4LS scheme in the small and large bandwidth limits. (a) Entanglement witness ($1/\xi^2$, solid) as a function of the squeezing parameter, r , for increasing number of qubits ($N = 2, 10, 50, 100, 200$) in the small photonic bandwidth limit, where $J_{m,n}^s \equiv 0$. In all the cases, the purity of the system is $\mathcal{P} \approx 1$. Inset: Dynamics of the entanglement witness ($1/\xi^2$) for the ensembles of qubits with a fixed random dispersion of qubit energies, $\Delta = 10\Gamma$, for the different number of qubits depicted in the main panel. (b) Entanglement witness ($1/\xi^2$, solid) and purity (\mathcal{P} , dashed) as a function of the parameter r for increasing number of qubits ($N = 2, 10, 50, 100, 200$) in the large bandwidth limit. The evolution of the collective dephasing mechanism, Γ_z , with the squeezing parameter is also plotted in solid black.

Recent experimental results [28,29] show level schemes in quantum dots similar to those required in our work. (iii) Markovian approximation. We require $\Gamma N \ll \omega_0$ in the 2LS scheme and $\Gamma N \ll \omega_{L1,2}, \omega_a$ in the 4LS case, such that the cooperative decay rate is much smaller than the transition frequencies; the latter determine the photonic bath memory time [30]. This condition is well satisfied in the case of optical transitions of quantum dots. (iv) Independent decay channels on each transition frequency. This is required for the 4LS's scheme in the large bandwidth limit, to obtain Eqs. (10) and (12), and is justified as long as $\Gamma N \ll |\omega_{L1} - \omega_a|, |\omega_{L2} - \omega_a|$. Since differences in the transition energies are of the order of millielectron volts, this condition imposes a restriction on the achievable rates for entanglement generation in our scheme. (v) Homogeneous couplings. So far we have neglected inhomogeneities in the couplings and qubit energies, which take the steady state out of the $|J, M\rangle$ basis. This may be a severe restriction in quantum optical solid-state devices. Although inhomogeneous broadening in solid-state setups is still of the order of millielectron volts for quantum dots [13] and microelectron volts for nitrogen vacancy centers [41], the feasibility of our proposal will benefit from current experimental efforts in the field.

We have carried out calculations to check the effect of experimental imperfections with a focus on an inhomogeneous random distribution of qubit energies, $\Delta\omega_j$, described by a term $H_{\text{inh}} = \sum_j \Delta\omega_j \sigma_j^z$ (with $\Delta\omega_j \in [-\Delta, \Delta]$). Exact calculations are very demanding; however, for a limited number of qubits $N = 2, 3, 4$, we are able to show that H_{inh} induces a dephasing time t_d , such that for $t > t_d$, spin squeezing is totally degraded in the 2LS scheme, or strongly decreases below its maximum value in the 4LS case (see Ref. [31] for details). In the 4LS scheme, one can use a bosonic approximation in the master equation ($\sigma_n \approx b_n$, with b_n a bosonic annihilation operator) and render the problem solvable in a low occupation limit $\langle \sigma_n^+ \sigma_n \rangle \approx 0$. This method has allowed us to study the scaling of the spin squeezing for large N . Our main result is that, under the effect of H_{inh} , the system reaches the steady-state spin-squeezing values, and after a time t_d , entanglement degrades down to a residual value. The robustness of the 4LS scheme increases for large N , since t_d grows with N . In the inset of Fig. 3(a) we show results for small values of r , which are particularly well described by the bosonization method. We confirm the same scaling with larger values of r with higher degrees of $1/\xi^2$ (see Ref. [31] for details). Our conclusion is that the 4LS is advantageous with respect to the 2LS, since it allows us to generate higher spin-squeezing values with d increasing with N .

In conclusion, we have proved that one-dimensional plasmonic [4,5] or photonic [6–10] waveguides can be used to correlate a large number of qubits by collective radiative decay. Our scheme is feasible in solid-state devices currently under investigation for quantum

information processing. Those ideas can be translated to circuit QED by controlling the qubit-field coupling (see Ref. [42]).

We acknowledge QUITMAD S2009-ESP-1594, MICINN-MAT2011-22997, CAM-S-2009/ESP-1503, FIS2009-10061, CAM-UCM/910758, RyC Contract No. Y200200074, and FPU Grant No. AP2008-00101. We thank to J. Miguel-Sanchez for useful discussion of the experimental conditions.

Note added.—During completion of this work we became aware of a theoretical preprint on atomic ensembles in single-mode optical cavities [43] related to our 4LS scheme. In our work we assume the continuum of modes in a one-dimensional waveguide, and thus we do not require the energetic resolution of a single cavity mode, which would hinder the scaling up of our scheme in solid-state setups with a large number of qubits.

-
- [1] A. Badolato, K. Hennessy, M. Atatüre, J. Dreiser, E. Hu, P. M. Petroff, and A. Imamoglu, *Science* **308**, 1158 (2005).
 - [2] K. Hennessy, A. Badolato, M. Winger, D. Gerace, M. Atatüre, S. Gulde, S. Fält, E. L. Hu, and A. Imamoglu, *Nature (London)* **445**, 896 (2007).
 - [3] D. Englund, B. Shields, K. Rivoire, F. Hatami, J. Vučković, H. Park, and M. D. Lukin, *Nano Lett.* **10**, 3922 (2010).
 - [4] A. V. Akimov, A. Mukherjee, C. L. Yu, D. E. Chang, A. S. Zibrov, P. R. Hemmer, H. Park, and M. D. Lukin, *Nature (London)* **450**, 402 (2007).
 - [5] A. Huck, S. Kumar, A. Shakoor, and U. L. Andersen, *Phys. Rev. Lett.* **106**, 096801 (2011).
 - [6] M. Lončar, D. Nedeljković, T. Doll, J. Vučković, A. Scherer, and T. P. Pearsall, *Appl. Phys. Lett.* **77**, 1937 (2000).
 - [7] Y. Vlasov, M. O'Boyle, H. H. F. and S. J. McNab, *Nature (London)* **438**, 65 (2005).
 - [8] E. Viasnoff-Schwoob, C. Weisbuch, H. Benisty, S. Olivier, S. Varoutsis, I. Robert-Philip, R. Houdré, and C. J. M. Smith, *Phys. Rev. Lett.* **95**, 183901 (2005).
 - [9] T. Lund-Hansen, S. Stobbe, B. Julsgaard, H. Thyrrstrup, T. Sünner, M. Kamp, A. Forchel, and P. Lodahl, *Phys. Rev. Lett.* **101**, 113903 (2008).
 - [10] A. Laucht, S. Pütz, T. Günthner, N. Hauke, R. Saive, S. Frédérick, M. Bichler, M.-C. Amann, A. W. Holleitner, M. Kaniber, and J. J. Finley, *Phys. Rev. X* **2**, 011014 (2012).
 - [11] A. Wallraff, D. I. Schuster, A. Blais, L. Frunzio, R.-S. Huang, J. Majer, S. Kumar, S. M. Girvin, and R. J. Schoelkopf, *Nature (London)* **431**, 162 (2004).
 - [12] O. Astafiev, A. M. Zagoskin, A. A. Abdumalikov, Y. A. Pashkin, T. Yamamoto, K. Inomata, Y. Nakamura, and J. S. Tsai, *Science* **327**, 840 (2010).
 - [13] A. Mohan, P. Gallo, M. Felici, B. Dwir, A. Rudra, J. Faist, and E. Kapon, *Small* **6**, 1268 (2010).
 - [14] A. Imamoglu, D. D. Awschalom, G. Burkard, D. P. DiVincenzo, D. Loss, M. Sherwin, and A. Small, *Phys. Rev. Lett.* **83**, 4204 (1999).
 - [15] M. B. Plenio, S. F. Huelga, A. Beige, and P. L. Knight, *Phys. Rev. A* **59**, 2468 (1999).
 - [16] F. Verstraete, M. M. Wolf, and J. I. Cirac, *Nat. Phys.* **5**, 633 (2009).
 - [17] H. Krauter, C. A. Muschik, K. Jensen, W. Wasilewski, J. M. Petersen, J. I. Cirac, and E. S. Polzik, *Phys. Rev. Lett.* **107**, 080503 (2011).
 - [18] A. Gonzalez-Tudela, D. Martin-Cano, E. Moreno, L. Martin-Moreno, C. Tejedor, and F. J. Garcia-Vidal, *Phys. Rev. Lett.* **106**, 020501 (2011).
 - [19] D. Martín-Cano, A. González-Tudela, L. Martín-Moreno, F. J. García-Vidal, C. Tejedor, and E. Moreno, *Phys. Rev. B* **84**, 235306 (2011).
 - [20] D. Dzotjan, A. S. Sørensen, and M. Fleischhauer, *Phys. Rev. B* **82**, 075427 (2010).
 - [21] K. Stannigel, P. Rabl, and P. Zoller, *New J. Phys.* **14**, 063014 (2012).
 - [22] R. H. Dicke, *Phys. Rev.* **93**, 99 (1954).
 - [23] M. Gross and S. Haroche, *Phys. Rep.* **93**, 301 (1982).
 - [24] R. H. Lehmberg, *Phys. Rev. A* **2**, 883 (1970).
 - [25] P. D. Drummond and C. H. J. J., *Opt. Commun.* **27**, 160 (1978).
 - [26] P. D. Drummond, *Phys. Rev. A* **22**, 1179 (1980).
 - [27] S. Schneider and G. J. Milburn, *Phys. Rev. A* **65**, 042107 (2002).
 - [28] J. M. Elzerman, K. M. Weiss, J. Miguel-Sanchez, and A. Imamoglu, *Phys. Rev. Lett.* **107**, 017401 (2011).
 - [29] K. M. Weiss, J. M. Elzerman, Y. L. Delley, J. Miguel-Sanchez, and A. Imamoglu, *Phys. Rev. Lett.* **109**, 107401 (2012).
 - [30] H.-P. Breuer and F. Petruccione, *The Theory of Open Quantum Systems* (Oxford University Press, New York, 2002).
 - [31] See Supplemental Material at <http://link.aps.org/supplemental/10.1103/PhysRevLett.110.080502> for details on the derivation of the master equation and numerical calculations including system imperfections.
 - [32] D. Martín-Cano, L. Martín-Moreno, F. J. García-Vidal, and E. Moreno, *Nano Lett.* **10**, 3129 (2010).
 - [33] F. Le Kien, S. D. Gupta, K. P. Nayak, and K. Hakuta, *Phys. Rev. A* **72**, 063815 (2005).
 - [34] D. E. Chang, L. Jiang, A. V. Gorshkov, and H. J. Kimble, *New J. Phys.* **14**, 063003 (2012).
 - [35] D. J. Wineland, J. J. Bollinger, W. M. Itano, and D. J. Heinzen, *Phys. Rev. A* **50**, 67 (1994).
 - [36] A. Sørensen, L.-M. Duan, J. I. Cirac, and P. Zoller, *Nature (London)* **409**, 63 (2001).
 - [37] M. Kitagawa and M. Ueda, *Phys. Rev. A* **47**, 5138 (1993).
 - [38] X. Wang and B. C. Sanders, *Phys. Rev. A* **68**, 012101 (2003).
 - [39] G. Lecamp, P. Lalanne, and J. P. Hugonin, *Phys. Rev. Lett.* **99**, 023902 (2007).
 - [40] X. Xu, Y. Wu, B. Sun, Q. Huang, J. Cheng, D. G. Steel, A. S. Bracker, D. Gammon, C. Emary, and L. J. Sham, *Phys. Rev. Lett.* **99**, 097401 (2007).
 - [41] Y. Kubo, I. Diniz, A. Dewes, V. Jacques, A. Dréau, J.-F. Roch, A. Auffeves, D. Vion, D. Esteve, and P. Bertet, *Phys. Rev. A* **85**, 012333 (2012).
 - [42] D. Porras and J. J. García-Ripoll, *Phys. Rev. Lett.* **108**, 043602 (2012).
 - [43] E. G. D. Torre, J. Otterbach, E. Demler, V. Vuletic, and M. D. Lukin, *arXiv:1209.1991*.